An Anisotropic Diffusion Approach for Early Detection of Breast Cancer

Marius George Linguraru, Michael Brady

▶ To cite this version:

AN ANISOTROPIC DIFFUSION APPROACH FOR EARLY DETECTION OF BREAST CANCER

Marius George LINGURARU*, Michael BRADY

University of Oxford, Medical Vision Laboratory, Ewert House, Ewert Place, Summertown, Oxford OX2 7BZ, United Kingdom
mglin@robots.ox.ac.uk

Abstract: The prevalence of breast cancer in the modern world has motivated the development of new tools to assist radiologists in their quest to detect malignancy as early as possible. Following the successful introduction of the screening programmes, science must provide effective clinical methods to detect cancer and improve life expectancy. Considerable research has been undertaken to this end, but the results still lack the robustness necessary for routine clinical applications. Mammographic images are difficult to interpret even by radiologists and this makes their task error prone. This paper presents a new approach to filtering breast images, which highlights the structures of anatomical interest. A method to detect calcifications has been explored. The approach is based on an edge preserving filtering with anisotropic diffusion. The algorithm makes use of the advantages offered by the h_{int} images, a normalised physical-based representation of the breast. The results are promising with excellent true positive rates in both detection of isolated coarse calcifications and microcalcifications with a very low number of false positives per image.

Key words: digital mammography, breast cancer, microcalcifications, h_{int} image representation, shot noise, anisotropic diffusion.

1. Introduction

1.1 The Impact of Breast Cancer

The incidence of cancer in the Western world is enormous. The impact that this fierce affliction has for a large percent of the population is a cultural phenomenon. *Fear of cancer* is an unfortunate reality that our auditive system has got used to! It has massive connotation for many domains, since *the hospital* lost its copyright for the term "cancer"' and now shares it with general sciences and even humanities, such as philosophy, literature and arts. Nevertheless, science is struggling to find new ways of improving worrying statistics, which show an increase in the impact that cancerous diseases are having especially over Europe and Americas.

Recent figures show that breast cancer is suffered by a high percent of the overall cancer incidence in women, where it accounts for approximately 25% of all female cancers. With about 600.000 new cases every year, breast cancer is second after lung cancer, the most feared form of cancerous death in women of all ages. The disease has a far higher incidence in Europe (especially Western Europe) and North America. In the far Orient and black Africa the mortality rate due to breast cancer is much lower, although there has been a substantial increase in the number of new cases. Such statistics represent intensive food for thought for researchers trying to trace genetic and environmental causes that lead to developing the disease.

Breast cancer's incidence is low in women under 30 years old and then increases with age. Between 40 and 50, women face a doubling of the rate of incidence which continues to increase over the age of 50, but more slowly. Younger women are encouraged to check the status of their breasts by simple palpation. Unfortunately, most women cannot reliably palpate a tumour smaller than 1 cm, therefore more examinations are required. In the UK, a screening programme is necessary for women over 50, since mammography is ineffective before menopause. There are several criteria that need to be fulfilled before starting a screening programme [8], such as:

- the disease to be screened must be very common and a treatment must be available for it, since there are very high costs involved and it would be of no use to look for a non-treatable affliction;
- the detection method must be robust, reliable and lead to good results for the overall screening process;
- must have high specificity;
- must be accepted by patients, since the method would not be cost-effective without a large number of patients to be examined.

The screening programme mainly represents a mean of detecting cancer signs from an earlier stage and subsequently improving the prognosis for patients. If a mammogram presents any features that seem suspicious to the radiologist, the patient will be asked to attend an assessment clinic where

more investigations will be performed by means of medical imaging and consulting. Figures show that 8% of women are recalled for further investigations, most of them not presenting any malignancy. The screening programme should, according to optimistic statements, almost double the chances of survival in women developing breast cancer. There is intensive debate as to whether the breast screening clinical assessments should be performed every two years instead of the three year period presently considered acceptable, as it has been noticed that the assessed women sometimes develop cancer over a period shorter than three years ("interval cancer").

When speaking about breast cancer, one generally refers to a set of breast afflictions, children of the same many-headed monster, which have one common wicked status: *the presence of malignancy*. Moreover, we are dealing with different stages of the same disease and the treatment given to affected women differs considerably from one stage to another. So does the prognosis, which represents a statistical measure of the chances of having a positive outcome of the treatment the patient is undergoing. The most relevant factors a doctor considers when deliberating on the prognosis are the size and type of the tumour, the presence of metastases, the stage of the disease, the status of the axillary lymph nodes and patient's age and medical condition.

1.1.1 A Brief Anatomy of the Breast

For a better understanding of the subject, we first overview the breast anatomy. The female breast has two separate functional parts:

- the milk-producing tissue (the epithelial tissue) which appears very dense in mammograms due to the high percent of calcium it contains;
- the other types of breast tissue, including water-dense non-fat tissue (which also appears light, but not as bright as calcium), breast fat-tissue (which is transparent in X-ray imaging and corresponds to the milk-producing tissue converted to fat after menopause), fascia (the connective tissue), and muscles.

Figure 1 shows a comparison between the appearance of the mammography of a breast of a young woman and an image of a breast of a post-menopausal woman.

The routes preferred by cancer in its spreading process are the blood and lymph vessels (which make the axillary nodes an important feature in signalling metastatic diseases), but the direct invasion of the surrounding tissue may have the same effect. Therefore, one would naturally speak about spreading (*invasive*) and non-spreading (*in-situ*) forms of cancer.
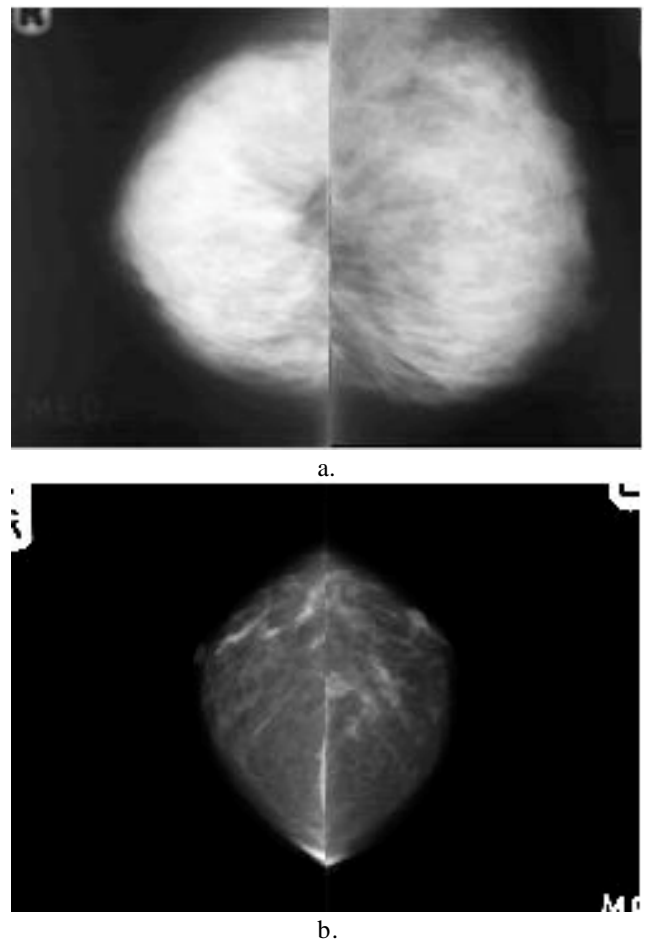

a.

b.

Figure 1. (a) A pair of mammograms taken from a young woman showing mainly dense tissue in the breast; (b) a pair of mammograms taken from a post-menopausal woman where the milk-producing tissue has converted to fat.

1.2 The Need for Image Segmentation

Image processing is a challenging but difficult task. Working with mammograms is especially complex due to the complicated appearance of the structures of interest in this particular type of image representation. Although a mammogram is a good *picture* of the breast, this is hardly sufficient when searching for small or complex anatomical parts, such as microcalcifications, masses or curvilinear structures in the process of early detection of breast cancer. Statistics show that approximately 25% of cancers are missed and about 80% of the biopsies are performed for benign cases. The complicated anatomy of the breast is an inevitable source of the highly textured structure of the mammograms. It provides a most difficult to analyse input for the radiologist, who is expected to distinguish very subtle abnormalities out of this mass of structural ambiguity. The variability between

any two different cases adds to the difficult task that the human decision maker faces.

1.2.1 Image Quality

The quality of the image depends on several physical factors. The most important are the different breast deformation during the compression process, the time of exposure, the breast thickness and various other imaging factors. Since the X-ray dosage cannot be too high, for patient safety reasons, there is a compromise between dosage and the signal-to-noise ratio (SNR) of the mammogram. This is even more degrading to the quality of the image, which must reflect the superimposed structures of the breast (a 3D structure) on a 2D projection. Noise is added to these features. This presentation of the mammogram could be easily reduced to that of a large textured noisy image, which still represents the best tool for early cancer detection to be used around the world. Section 2 will present some major improvements in image acquisition developed by the Medical Vision Laboratory at the University of Oxford.

1.2.2 Digital Mammography

Mammography is predominantly film-based and represents the outcome of three subsequent processes, image acquisition, image storage and viewing. The overall process is dependent on the same medium, the film. Although many technical problems have retarded the digitisation of mammography, and still prevent it from being used widely, directly digital mammography is now available [8]. The digital systems make a clear distinction between image acquisition, image storage and image visualisation. There are several clear advantages that digital imaging has to offer:

- *digital image acquisition* is expected to reduce the X-ray dose in the imaging process, leading to less risk for the patient; it also improves the contrast resolution;
- *digital image storage* reduces the cost of the operation since it does not require film and chemicals, provides fast and reliable retrieval from the archive and allows the collection of large image databases;
- *digital image visualisation* enables the use of Computer Aided Diagnosis (CAD) for automatic detection, data documentation and the universe of image processing; it greatly improves the quality of the displayed image over that of the rigid film.

Early detection can be accomplished only with high quality detection and processing tools in the different levels of the screening programmes. Directly digital mammography is the new trend in X-ray mammography and will bring serious improvements in the development of screening programmes. The *soft-copy reading environment* [8], a computer workstation which displays digital mammograms for the radiologist to read, is the tool that will make digital mammography available in hospitals for much better results in detecting the structures of interest within the breast.

1.2.3 Future Trends

There are several implemented techniques, which bring improvements in the field of medical imaging. Most of them have proved not to be satisfactory for the purpose that they are used, such as automatic detection and working with mammograms. Moreover, although the resulting images they provide look quite impressive, it has not been definitely proved that radiologists work better on these images. Therefore, there is sufficient room for improvements and further developments in image processing. Some present trends in the field include:

- the development of soft-copy reading workstations [8], as the tool for the future use of digital mammograms;
- friendlier user-interfaces (touch-screen, automatic report generation, robust display) which would only require a minimal intervention from the human factor involved, the radiologist;
- the development of training-systems with immediate feedback and the use of larger databases;
- the development of real-time applications for making the best use of the image processing methods in clinical applications;
- software integration of the existing algorithms is an inherent condition in building strong performant medical systems;
- finding more reliable, more robust and faster image processing algorithm that will have a great impact on the future of medical analysis.

2. H_{int} Model

The h_{int} representation [10] is a physical-based approach to mammographic analysis, an image normalisation method based on a complete understanding of the imaging process. Since the quality of mammograms is so highly dependent on the imaging conditions, the h_{int} model is an alternative *quantitative* representation of the breast tissue. Figure 2 shows a depiction of the h_{int} surface of a breast.

The intensity or attenuation value of a pixel in a mammogram is determined by the quantity of X-ray beam absorbed by the tissue present between the X-ray source and the respective pixel. The h_{int} value of a pixel represents the thickness of the breast tissue of interest underlying between the X-ray source and the actual pixel. By interesting tissue one must consider the non-fatty tissue present in the breast, such as glandular, cancerous and fibrous tissue, which have high attenuation. Hence, the h_{int} representation is not dependent on the imaging procedure the same way the intensity value is. Other types of tissue present within the breast are the fatty tissue with low attenuation and the

calcifications with very high attenuation, since they contain a concentrated level of calcium. They lead to the definition of h_{fat} and h_{calc}, the thickness of the fatty tissue and calcification. Calcifications are very small anatomical features of the breast, so we can compute the total thickness of the compressed breast with:
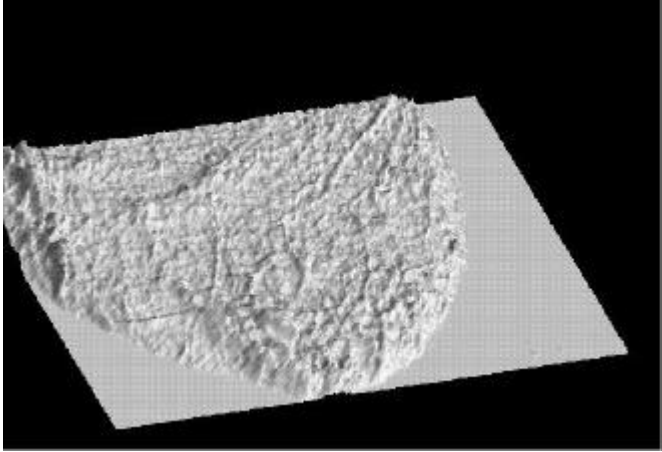
$$H = h_{int} + h_{fat} \tag{1}$$

Figure 2. A depiction of the h_{int} surface of a breast

2.1 Generating H_{int}

Although formula (1) has a very simple appearance, the computation of h_{int} is a rather complex process. Here are the steps to be followed to generate h_{int} [10]:

- convert the pixel value $P(x,y)$ into film density $D(x,y)$ and deblur; this is achieved by considering the linear relationship between $P(x,y)$ and $D(x,y)$ followed by the use of the modulation transfer function;
- convert the film density $D(x,y)$ into energy imparted to the intensifying screen $E_{pse}{}^{imp}(x,y)$; the film-screen calibration data is relevant for this purpose; the energy imparted image appears as an inverted version of the density image, where dark parts correspond to high energies;
- compensate $E_{pse}{}^{imp}(x,y)$ for the intensifying screen glare by using the point-spread function of the intensifying screen;
- compensate $E_{pse}{}^{imp}(x,y)$ for the anode-heel effect and diverging X-ray beam, by knowing the variation between the incident photon flux between different spatial locations on the film;
- estimate the scattered radiation $E_s{}^{imp}(x,y)$, since this component of the imparted energy contains no information about the breast tissue but influences the neighbourhood of the pixel;
- estimate the extra-focal radiation $E_e{}^{imp}(x,y)$ component, which is relevant at the curved breast edge where photons arriving with low angles can reach the intensifying screen;

- compute the primary radiation $E_p{}^{imp}(x,y)$;

$$E_p{}^{imp}(x,y) = E_{pse}{}^{imp}(x,y) - E_e{}^{imp}(x,y) - E_s{}^{imp}(x,y) \tag{2}$$

- convert $E_p{}^{imp}(x,y)$ into h_{int} using the conversion equations developed by Highnam and Brady [10].

2.2 Strengths of the H_{int} Model

The h_{int} representation is a robust and reliable method, resulting in a floating point form, which corresponds to the thickness of interesting tissue in the breast. By removing most of the unwanted effects of the imaging process, such as glare, scatter radiation, anode-heel effect and extra-focal radiation, the output of the method presents a much more adequate representation of the real anatomical structure of the breast. Hence, the h_{int} representation of the breast is mainly a 3D surface built from the h_{int} values of the image pixels. By removing the image parameters, the h_{int} images stand as normalised images of the breast.
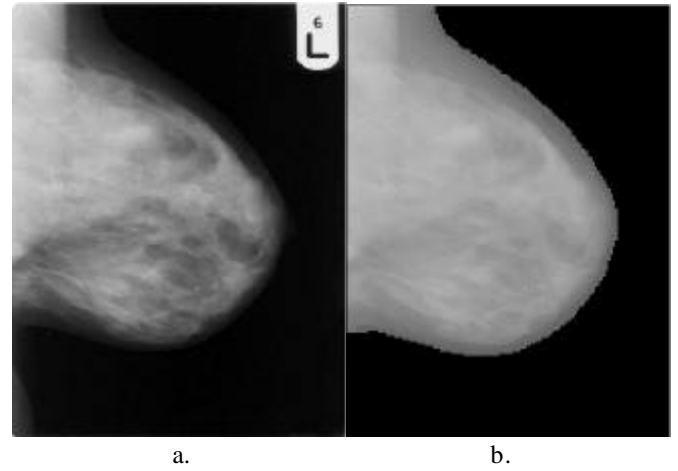

a.   b.

Figure 3. (a) An original mammogram and (b) its corresponding h_{int}. image.

An h_{int} representation can be easily visualized as an image, since the h_{int} values are in float format, where brighter parts correspond to thicker parts of the breast or calcifications as in Figure 3. Moreover, the depicted surface of an h_{int} representation of the breast can show important anatomical features, such as masses as hills in a less dense background, while the background is mainly flat.

3. Abnormal Structures in Breast Anatomy

This section aims to overview briefly some of the most relevant papers that relate to the subject of this research. Section 3.1 presents the most important achievements to date in detecting microcalcifications. The detection and

classification of tmours are open subjects for future research. Section 3.2 reviews the state of the art in the detection and classification of masses in X-ray mammography.

3.1 Detection of Microcalcification

Microcalcifications represent some of the earliest signs of breast cancer and they account for half of the non-palpable lesions that appear in mammograms. Calcifications are either warnings of malignancy or just benign signs of aging. They are encountered in approximately 25% of mammograms and appear as bright spots or clusters of such spots, due to the high density of calcium. To differentiate malignant from benign microcalcifications, radiologists believe that they take into consideration several criteria, such as shape, size and arrangement.

According to their size, calcifications can be classified into macrocalcification or coarse calcifications (when their size usually exceeds 1 mm) and microcalcifications. While it is believed that large single regular-shaped calcifications are benign, small clustered whorled calcifications are more likely to signify malignancy, as noticed by Caseldine *et al}* [3] and Le Gal *et al.* [9]. Although the detection and classification of calcifications are two fields that have improved significantly in recent years, there is still no robust differentiation between benign and malignant calcifications and a large enough number of calcifications are still not detected by radiologists or by detection algorithms. Figure 4 shows two examples of samples of mammograms containing calcifications.
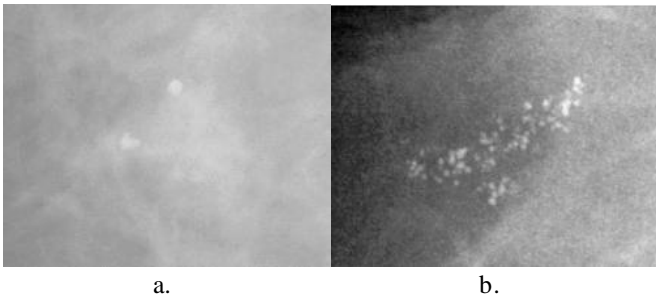

Figure 4. (a) A mammogram sample showing two isolated coarse calcifications; (b) a microcalcification cluster.

The aim of automatic detection is to find a sufficiently reliable algorithm to be used in clinical practice. Such algorithms are meant to assist the radiologist in making decisions and to improve the overall sensitivity (the proportion of true positives, TP) and specificity (1-the proportion of false positives, FP) of the detection process. Some of the factors that drastically influence the TP and FP figures are:
- the variability of the anatomy of the breast; every mammogram has different features related to different

tissue types and correspondingly variable brightness in the mammographic appearance;
- the imaging conditions, such as shot noise, patient movement, low contrast in mammograms, due to low X-ray dosage and glare;
- faint microcalcifications lost in a dense background, the superposition of certain breast structures.

In order to overcome the above-mentioned compromising factors, most of the conventional detecting algorithms comprise three main stages:
- a pre-processing step based on filtering the image; the filter is meant to detect and remove the noise and enhance the structures of interest, the microcalcifications; Chan *et al}* [5] and Nishikawa *et al}* [20] use a difference image, the result of subtracting a signal-enhanced image by a signal-suppressed image;
- a segmentation step based on adaptive thresholding or local contrast; Nishikawa *et al.* use both global thresholding and morphological erosion;
- a clustering step using a fixed size kernel to eliminate noise points and isolated calcifications and identify clusters.

Although most of the conventional detection methods are based on the above algorithm, the literature includes a couple of novel detection methods. Yam *et al.* [26], [27] present a physics-based approach, which uses both grey level and h_{int} images. The method extracts regions corresponding to the size of microcalcifications that satisfy a criterion related to the change of surface with the height. The ratio between the actual volume of the extracted blob and the volume of the interesting tissue (h_{int}) is the second feature that is introduced.

Another innovative detection method is Karssemeijer's statistical approach [12],[13]. An adaptive noise equalisation algorithm was developed to deal with the variation of noise characteristics in an image. It makes use of Bayesian techniques combined with Markov random fields.

3.2 Detection of Masses

Masses represent a special category of breast abnormalities and their detection is a subject that is intensely debated and researched in digital mammography. Generally, masses appear as bright regions in a mammogram with rather well contoured boundaries. Nevertheless, it is particularly difficult to identify some mass-like structure, since the interesting dense tissue within the breast may have similar density values and overlap with masses. In the above-mentioned case, it is a real challenge to identify the shape and the edges of the mass. An important source of FPs is the overlapping of two dense regions, due to the projective nature of a mammogram, which would look brighter that its surroundings and be confused with a mass. For this reason, two views are taken from the breast, a cranio-caudal (CC) and a medio-lateral-oblique

(MLO) view. Figure 5 shows two examples of samples of mammograms containing masses.
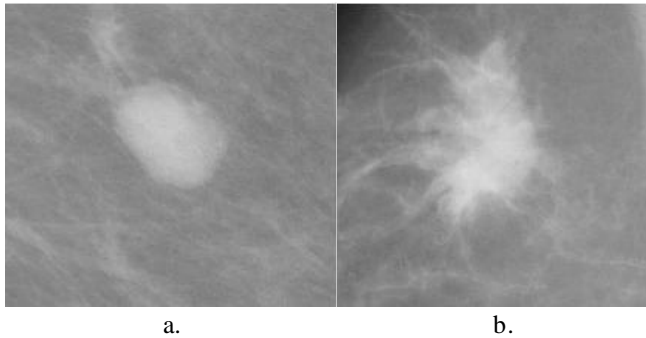

a.   b.

Figure 5. (a) A mammogram sample showing a benign mass; (b) a malignant mass.

When related to masses, automated image analysis relies on three main applications:

- locating abnormal regions in a single mammogram, when, as a result of several features calculated, possibly pathological regions of the breast are extracted and pointed out to the radiologist;
- matching bilateral pairs, making use of the same-view left and right breast mammograms of the same woman at the same time, acknowledging the approximate symmetry of the two breasts;
- matching temporal pairs, using the same-view of the same breast mammograms of the same woman at two different times, searching the major changes that appear between the two mammograms; [19]

Amongst the most relevant achievements in detecting breast lesions, te Brake and Karssemeijer [2],[14] consider the irregular shape that so-called speculated masses may have and the often noted stellate appearance of them, as radiating patterns of linear spicules. This method uses gradient operators for determining the relevant line orientation. Two features are considered: the total number of pixels with an intensity gradient pointing to a centre and the likelihood of having found a speculated structure, which becomes higher with the increasing number of directions in which pixels are oriented towards a region.

Chan *et al.* [6],[22] use a rubber-band-straightening transform (RBST) to transform the band of pixels surrounding a mass into a Cartesian plane (the RBST image), which has the advantage of making the mass margins almost parallel, with spicules to perpendicular the length of the rectangle. A large number of features are computed and the most relevant of them for used for Fisher's linear discriminant that will conclude with the likelihood of malignancy.

Highnam and Brady [9] comment on the advantages of using h_{int} representations in the way that a mass would correspond to a hill-like structure surrounded by a smoother

region corresponding to fibroglandular tissue. The ultimate aim of the detection of masses is their interpretation; therefore, the shape and arrangement of the salient region are relevant features in this process.

4. A Review of Anisotropic Diffusion

It has been often proved that filtering methods can substantially improve the quality of the image of interest by means of extinguishing artefacts and unwanted information from the original image, but also simplifying the appearance of otherwise complicated anatomical structures. The notion of image filtering has already been encountered in the previous section as an image pre-processing step used by some of the overviewed algorithms. Conventional filtering methods include a background smoothing stage (convolution with a low pass filter) followed by enhancement of the structures of interest (high pass filtering) and the subtraction of the two newly obtain images. This method could not deal with the large variability of the anatomical features that must be considered.

There are numerous algorithms based on evolving partial differential equations (PDE) for noise removal and image enhancement, but few of them have been previously tested on medical imaging. Furthermore, the extent of applying PDE filters to medical images seems to be generally related to ultrasound and MRI.

Anisotropic diffusion has its origins on the classical nonlinear diffusion filter developed by Perona and Malik in 1987 [21], which is based on a PDE in divergence form. It is the cornerstone for new developments in multi-scale image analysis aiming to simplify the image appearance while enhancing structures of interest, such as edges or coherent structures.

4.1 The Diffusion Process

One of the most commonly used methods for smoothing an image $f : R^2 \to R$ is by convolving it with a Gaussian with standard deviation s:

$$K_s(x) = (1/2p\ s^2) \bullet \exp(-/x/^2/2\ s^2) \qquad (3)$$

The image f is transformed into a family of gradually smoother versions for a higher number of iterations ($t>0$). An increasing scale will simplify the appearance of the original image. There are several limitations of this method, as observed in [25]:

- although convolution with a Gaussian reduces noise, it also blurs important anatomical structures of the images, such as edges;
- linear diffusion dislocates edges when changing from finer to coarser scales.

The diffusion process was proposed as an alternative to smoothing images by a Gaussian kernel, which does not preserve edges. Since it derives from a process of equilibrating concentration differences, it can be expressed through a continuity equation of Fick's law [25]:

$$j = -D \cdot \tilde{N}u \qquad (4)$$
$$\delta_t = \mathrm{div}(D \cdot \tilde{N}u) \qquad (5)$$

D is called the *diffusion tensor*, a positive definite symmetric matrix which represents the relation between the concentration gradient $\tilde{N}u$ and the flux which aims to compensate this gradient (4). In image processing, the concept of concentration is replaced by that of grey level. The diffusion tensor may be replaced by a positive scalar-valued *diffusivity g*. If j and $\tilde{N}u$ are parallel, the diffusion is called *isotropic*. In the *anisotropic* case, j and $\tilde{N}u$ are not parallel. Equation (5) is called the *diffusion equation*. If the diffusion tensor is space-dependent, then the diffusion is called *inhomogeneous*, while a constant diffusion tensor is related to a *homogeneous* diffusion.

In order to overcome the correspondence problem (the coarse-to-fine tracking difficulties), the inhomogeneous linear diffusion filtering introduces $|\tilde{N}f|$ as edge detector, where high values of the detector indicate the presence of edges in the image. The diffusivity function g was set to:

$$g(|\tilde{N}f|^2) = 1/\mathrm{sqrt}(1+|\tilde{N}f|^2/I^2) \qquad (6)$$

and the diffusion equation reduces to:

$$d_t u = \mathrm{div}(g(|\tilde{N}f|^2)\ \tilde{N}u) \qquad (7)$$

Introducing a feedback in the diffusion process, by adapting the diffusivity to the gradient of $u(x,t)$ -- the actual image, rather than the original $f(x)$ -- the diffusion equation becomes nonlinear and therefore the diffusion filtering will be nonlinear and isotropic:

$$d_t u = \mathrm{div}(g(|\tilde{N}u|^2)\ \tilde{N}u) \qquad (8)$$

The Perona-Malik Model [21] represents the first nonlinear diffusion filter. It provides stable edges over a long number of iterations based on a rapidly decreasing diffusivity, but will only enhance those edges for which the gradient is larger than the contrast parameter *?*.

$$g(|\tilde{N}f|^2) = 1/(1+|\tilde{N}u|^2/I^2) \qquad (? > 0) \qquad (9)$$

Catté *et al.* [4] introduced the Gaussian convolution of *u*: $u_s = K_s * u$ and the result of it was:

$$d_t u = \mathrm{div}(g(|\tilde{N}u_s|^2)\ \tilde{N}u) \qquad (10)$$

This new form of the diffusion equation solved the spatial regularizing problem of the inhomogeneous filtering, meaning that the solution of the nonlinear filtering method of images aims to a steady state. Moreover, a new parameter is introduced in the process, the *scale parameter* s. The process is now controlled by the three parameters, *t(time)*, *?(contrast)* and *s(scale)*, which tremendously reduce the impact of the choice of diffusivity over the whole process and make the use of it more flexible and robust. Although the contrast parameter will work similar to the Perona-Malik model, the scale parameter will make the filter less sensitive to small-size structures, such as noise, by increasing the kernel of the Gaussian s.

4.2 Nonlinear Anisotropic Diffusion

The main improvement introduced by the nonlinear anisotropic filters is the smoothing along the isophote and not across it when the value of the gradient is large [15]. While for low gradients smoothing is performed in the usual way, at edges diffusion is inhibited. Weickert [24],[25] introduces a system of eigenvectors *v1, v2* of the diffusion tensor *D. v1* and *v2* are orthonormal and

$$v1 \parallel \tilde{N}u_s, \qquad (11)$$

$$v2 \perp \tilde{N}u_s \qquad (12)$$

The corresponding eigenvalues are:

$$I_1 = g(|\tilde{N}u_s|^2), \qquad (13)$$

$$I_2 = 1. \qquad (14)$$

In general $\tilde{N}u_s$ is not parallel to one of the eigenvectors of D for $\sigma > 0$ and Weickert's model behaves really anisotropically. If σ tends to 0, the process tends to behave like the classical Perona-Malik model.

The edge-enhancing diffusion model proposed by Weickert is the one used in our initial experiments, where the diffusion across edges is performed according to the following eigenvalue:

$$I_1 = \begin{cases} 1 & |\tilde{N}u_s| = 0, \\ 1 - \exp(-3.31488/(|\tilde{N}u_s|/I)^8) & |\tilde{N}u_s| > 0. \end{cases} \qquad (15)$$

An example showing different stages of applying anisotropic diffusion to a sample of mammogram displaying a large microcalcification and some noise is shown in Figure 6.
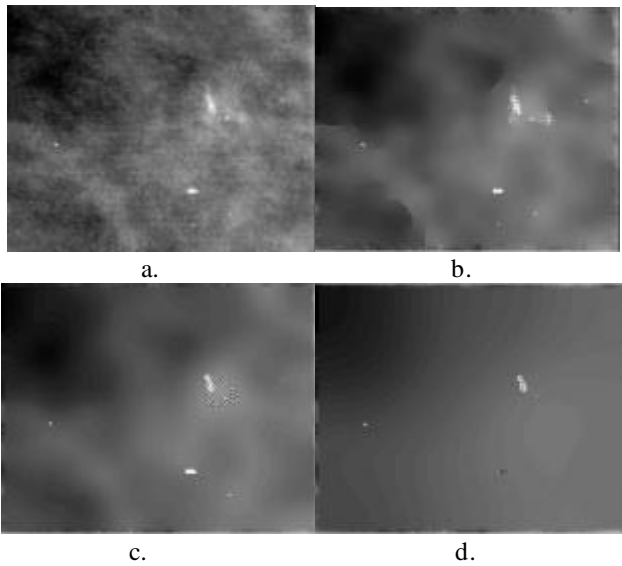
Figure 6. (a) The original sample of a mammogram with a large calcification on the upper-right side; (b) the diffused image with k=5, s=0.6 and t=20; (c) the diffused image with k=5, s=0.5 and t=20, where only small structures are kept and their edges enhanced; (d) further diffusion the image of (c) k=5,s=0.5 and t=500, the large bit of noise if removed.

4.3 Discussion

Anisotropic diffusion overcomes some major limitations of linear and nonlinear isotropic filters:

- enhances noisy edges and flow-like structures (would be useful in the detection of curvilinear structures);
- inhibits diffusion at edges;
- more flexible due to the larger number of parameters, but not large enough to alter the robustness and accuracy of this method;
- converges to a steady state for $t \to \infty$ respecting a maximum-minimum principle;
- its solution is unique and continuously dependent on the initial image.

The use of anisotropic diffusion, as observed in [25], spreads from computer aided quality control to post-processing fluctuating data, target tracking in infrared images and blind image restoration, to only enumerate some applications. But most applications are concerned with filtering medical images, mainly ultrasound and magnetic resonance images.

It is however not sufficient to use ``blind'' filtering methods when the features we need to preserve in an image are so precise and specific. The use of it *a priori* or even *a posteriori* knowledge in the diffusion process must be a future trend in the use of PDE-based filters, a field with continuous evolution which has to bring many advantages in the overall development of medical vision.

5. Filter Model

One of the major characteristics that we use in approaching microcalcification detection is the genuine difference that should be visible in the shape of microcalcification versus noise in mammographic imaging. While microcalcifications are anatomical structures with slightly blurred edges, which appear in mammograms due to the effect of X-ray beams passing through the breast anatomical structure, noise tends to have extremely sharp edges, as in Figure 7.
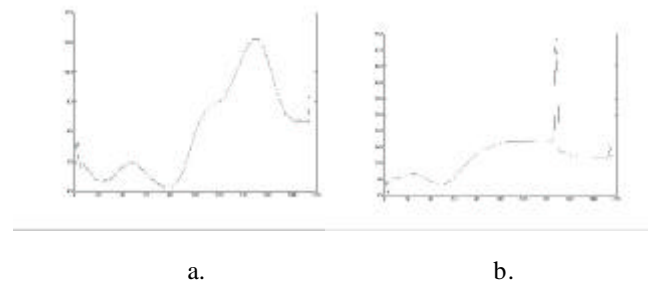

Figure 7. (a) The plot of a filtered intensity image containing a microcalcification at position 150; (b) the plot of a filtered image containing noise at position 147.

The appearance of h_{int} images would be extremely noisy mainly due to the removal of the glare effect, extra-focal and scattered radiation (which accounts for up to 40% of the total radiation exiting the breast). Although calcifications are small structures and they may be computationally omitted, the high attenuation of calcium makes them stand as a definite exception in the h_{int} representation. Since microcalcifications are high in h_{int} images, only the most prominent spots of noise may lead towards FPs, the smaller ones being easily removed by the diffusion process.

We chose an anisotropic diffusion-based filter, which attempts to blur the input mammographic image while preserving significant intensity changes. The process relies on the use of a set of different parameters, e.g. time (*t*), contrast (*k*), size (*s*), and it is critical to find the right choice of parameters that will lead to good repeatable results. The nonlinear anisotropic diffusion technique proves to be highly flexible de to the variability of its parameters which help in covering a rather extensive set o possibilities with respect to the output one can get by filtering medical images, as Table 1 shows. The diffusion tensor for the anisotropic filtering is based on Weickert's approach having the corresponding eigenvalues, λ_1 and λ_2 in (16), where u_s represents the Gaussian convolution of the original image u.

$$I_1 = \begin{cases} 1 & |\nabla u_s| = 0, \\ 1 - \exp\left(\dfrac{-1}{\left(|\nabla u_s|/k\right)^8}\right) & |\nabla u_s| > 0. \end{cases} \qquad (16)$$

$$I_2 = 1$$

Table 1

	Blur	Anatomical features	Edges
$k\nearrow$	$\nearrow$	$\searrow$	$\searrow\searrow$
$s\nearrow$	$\nearrow$	$\searrow$	$\searrow$
$t\nearrow$	$\nearrow$	$\searrow\searrow$	Well preserved

5.1 Diffusion and Surface Plots

We show some results from applying non-linear anisotropic diffusion filtering on samples of h_{int} representations of real mammograms containing microcalcifications in Figure 8. They demonstrate the accurate effect of de-noising h_{int} images performed by our method while preserving only calcifications and significant noise points. We also considered images with very high likelihood to present false positives (FPs). Such an example is presented in Figure 9.

a.   b.

c.   d.
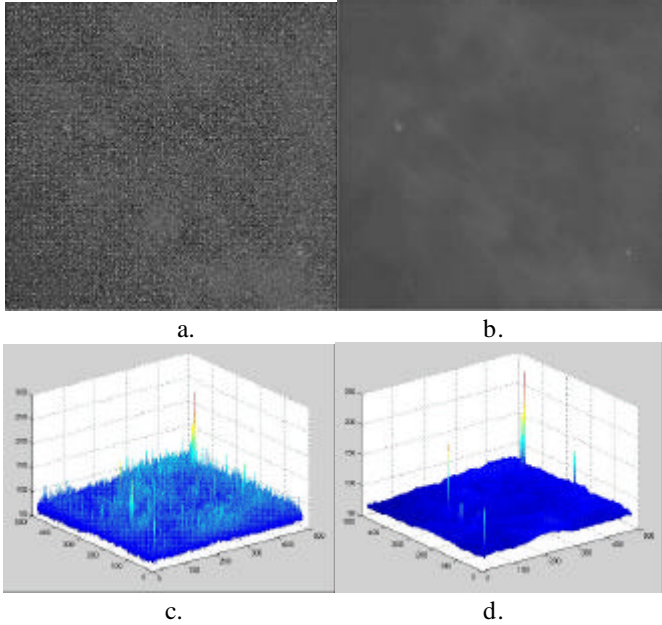
Figure 8. (a) A pre-processed h_{int} image containing a microcalcification on the left side and a large spot of noise on the lower right side; (b) the diffused version of the (a) image with k=15, s=0.6 and t=5; (c) the surface of the original h_{int} image in (a)with highly noisy appearance; (d) the surface of the diffused h_{int} image, the microcalcification appears as a hill with smoother edges than those of noise.

a.   b.

c.   d.
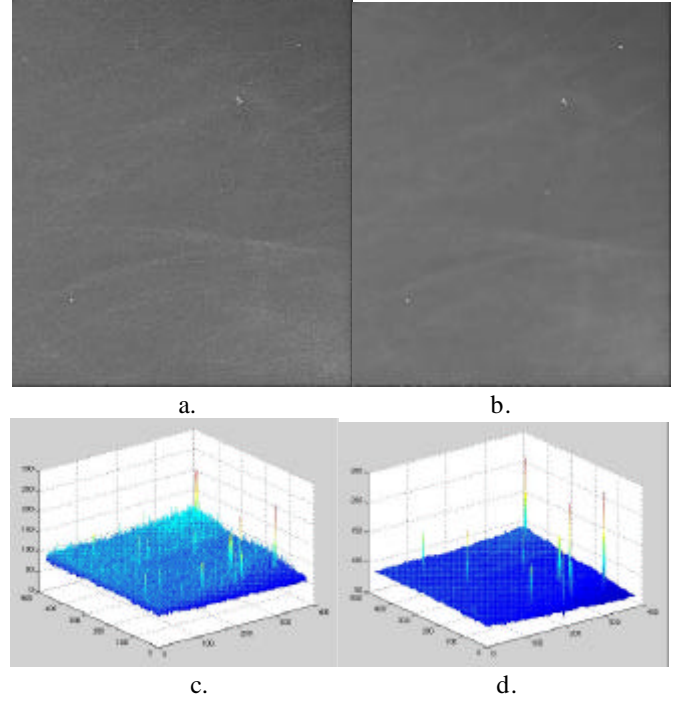
Figure 9. (a) The original pre-processed h_{int} image containing only noise structures; (b) the diffused version of the (a) image with k=15, s=0.6 and t=3; (c) the surface of the original h_{int} image in (a); (d) the surface of the diffused h_{int} image, where all structures have very sharp edges and are labelled as noise.

5.2 First Results

The detection method, for both calcifications and noise was based on the association one can make between the original h_{int} mammograms containing the structures of interest and the surface we built from the filtered images after just a few iteration steps. The surface we present would show either hill-shaped structures for microcalcifications or sharp-edged formations for noise in the locations corresponding to the structures of interest. The algorithm was tested initially on a set of 13 samples of average 32-bit h_{int} mammograms at 50 mm resolution containing 10 pre-labelled coarse calcifications and several artefacts. Samples were preferred, rather than whole mammograms, in order to reduce processing time. All the calcifications were correctly detected. No FPs were detected during our initial experiments. The free-response receiver operating characteristic (FROC) curve is shown in Figure 10a.

The algorithm was further tested on a set of 20 samples of 32-bit h_{int} mammograms at a resolution of 50 mm containing 27 pre-labelled isolated microcalcifications and various bits of noise. The TPs fraction was 92.6% for a number of 0.1 FPs per image. We further applied an implementation of Yam *et al.*'s algorithm on the filtered images of the same set of microcalcifications. We obtained a 100% fraction of TPs with a

number of 0.3 FPs per image. The FROC curve of the detection using the combination of the anisotropic diffusion filter and the algorithm implemented by Yam *et al.* (1999) is shown in Figure 10b.
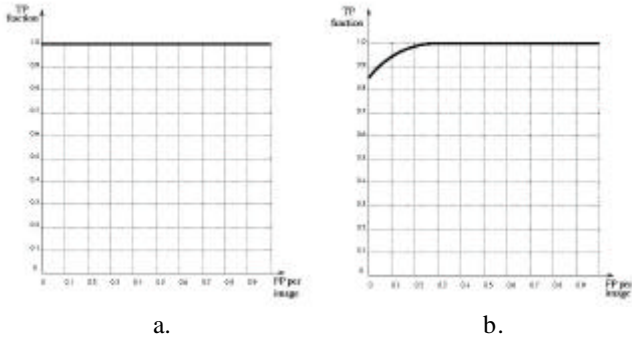

a.   b.

Figure 10 . (a) The FROC curve for the set of coarse calcifications; (b) the FROC curve of the combined detection method for the set containing different types of microcalcifications.

5.3 A Non-Parametric Approach

We designed an adaptive Gaussian derivative filter to apply to the de-noised, glare-removed h_{int} images, which results in a gradient map (Figure 11.b) that highlights suspicious regions as regards to microcalcification detection. The same filter outputs the value of k for the subsequent diffusion. Having the gradient map and the value of k, *w*e apply the anisotropic diffusion filter to the h_{int} image over a constant number of iterations t, with a pre-defined value of s and the corresponding value of k. The new image will generally be blurred (Figure 11.c), excepting some suspicious regions which will have their edges preserved. With the diffused images ready, we need to ensure that the artefacts emphasised in the gradient maps will be eliminated. A new filtering step is introduced at this stage to actually depict the microcalcifications in the processed image. It is based on the same computation as the anisotropic diffusion, but also incorporates some adaptive thresholding suited to the image characteristics and the properties of microcalcifications. This last filter will conclude with a black-and-white-map-of detection (BWMD – Figure 11.d).

In summary, our method uses three filters in sequence:
- an adaptive Gaussian filter;
- an anisotropic diffusion filter;
- an adaptive thresholding filter.

The method eliminates the initial parametric dependence and improves the overall robustness of the detection. We show three examples of detection: Figure 11 – the detection of a Ductal Carcinoma In Situ; Figure 12 – the detection of subtle microcalcifications; Figure 13 – avoiding FPs in detection by eliminating curvilinear structures (CLS) [7],[16].
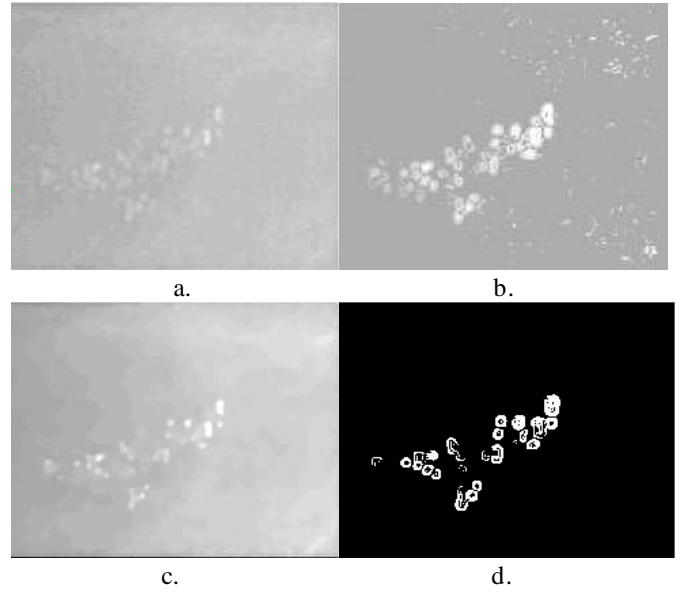

a.   b.

c.   d.

Figure 11. (a) An h_{int} sample containing a Ductal Carcinoma In Situ; (b) the gradient map of the (a) image with k=3; (c) the diffused image of (a); (d) the BWMD where the white regions correspond to calcium.

a.   b.

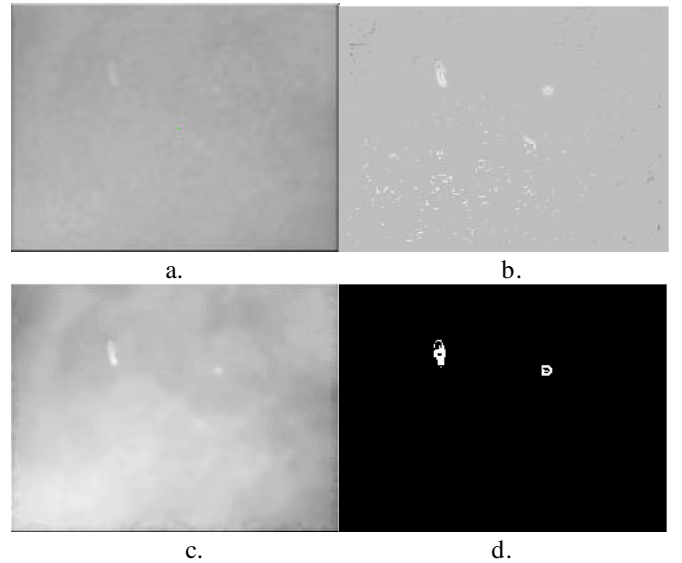c.   d.

Figure 12. Shows a difficult case of detection: (a) an h_{int} sample containing two subtle calcifications; (b) the corresponding gradient map; (c) the diffused image of (a) after using the computed value of k; (d) the BWMD with the depiction of the two microcalcifications.

The overall detection rate for microcalcifications became 91.3% TPs for a number of 0.2 FPs per image. Although the detection rate is slightly lower than in some of our previous experiments, this is the price to be paid for improving robustness.
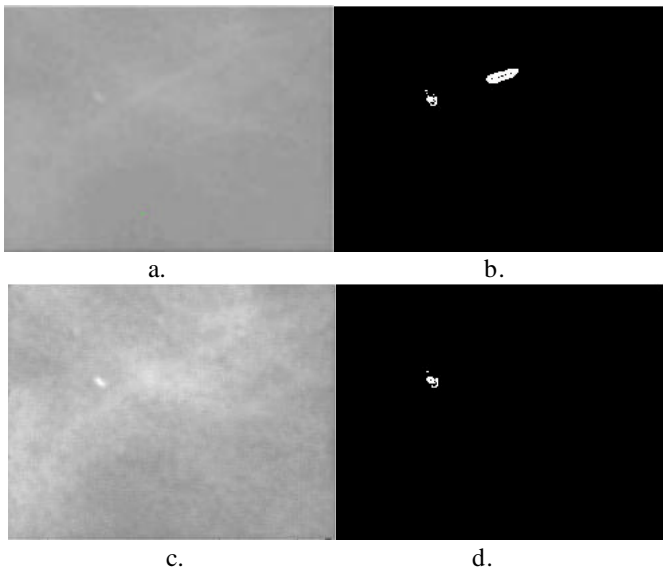
Figure 13. (a) An h_{int} sample containing one subtle microcalcification and a prominent CLS; (b) the BWMD of (a) showing an FP; (c) the same image as (a) after CLS removal and contrast enhancement; (d) the BWMD of (b) with the correct detection of the microcalcification.

6. Further Work

- Breast Edge Correction: the high gradient value around the boundary of the breast is a major source of errors; the solution would be bringing the background to an h_{int} value similar to that of the average breast tissue.
- Shot Noise Removal: shot noise is the major source of errors in the detection of microcalcifications; the h_{int} generation can detect shot noise and it can be therefore extracted by interpolation from the images we use, reducing the number of FPs.
- Wavelet Implementation: anisotropic diffusion is not sensitive to extremely small structures, therefore, by using wavelets we should improve the performance of the algorithm in dealing with very small salts of calcium; a combination of anisotropic diffusion and wavelets could be the key to our problem. While our current method could detect the general shape of a cluster and most of its calcifications; further developments should search within the boundaries of the cluster for particularly small and faint microcalcifications.

References

[1] C.M. Bishop -- *Neural Networks for Patters Recognition*, Oxford University Press, 1995.

[2] G.M. te Brake, and N.Karssemeijer – *"Single and Multiscale Detection of Masses in Digital Mammograms"*, in IEEE Transactions on Medical Imaging, vol. 18, pp. 628-639, 1999.

[3] J. Caseldine, R. Blamey, E.J. Roebck, and C. Elston – *Breast Disease for Radiographers*, Wright, 1988.

[4] F. Catté, P.L. Lions, J.M. Morel and T. Coll – *"Image Selective Smoothing and Edge Detection by Nonlinear Diffusion"*, in Numerical Analysis , vol. 29, pp. 182-193, 1992.

[5] H.P. Chan, K. Doi, S. Galhorta, C.J. Vyborny, H. MacMahon, and P.M. Jokich -- *"Image Features Analysis and Computer-Aided Diagnosis in Digital Radiography: 1.Automated Detection of Microcalcifications in Mammograms",* in Medical Physics, vol. 14, pp. 538-548, 1987.

[6] H.P. Chan, B. Sahiner, M.A. Helvie, N. Petrick, M.A. Roubidoux, T.E. Wilson, D.D. Adler, C. Paramagul, J.S. Newman, and S. Sanjay-Gopal – *"Improvements of Radiologists' Characterization of Mammographic Masses by Using Computer-aided Diagnosis: An ROC Study"*, in Radiology, vol. 212, pp. 817—827, 1999.

[7] C.J. Evans – *"Detecting and Removing Curvilinear Structures from Mammograms",* Internal Report, Department of Engineering Science, University of Oxford, 2001.

[8] C.J.G. Evertsz, A. Boedicker, S. Bohnenkamp, D. Dechow, L. Berger, U.Weber, C. Beck, J. Hendriks, N. Karssemeijer, M. Brady, H. Jurgens, and H.O Petgen -- *"Soft Copy Environment for Screening Mammography – SCREEN",* in M.J. Yaffe editor, International Workshop on Digital Mammography 2000, pp. 566-572, Medical Physics Publishing Madison, 2000.

[9] M. Le Gal, L. Ollivier, B. Asselain, et al. – *"Mammographic Features of 455 Invasive Carcinomas",* in Radiology, vol. 212, pp. 817-827, 1999.

[10] R.P. Highnam, and J.M. Brady -- *Mammographic Image Analysis,* Kluwer Academic Publisher, 1999.

[11] R.P. Highnam, J.M. Brady, and R. English – "Detecting Film-Screen Artifacts in Mammography using a Model-Based-Approach", in IEEE Transactions on Medical Imaging, vol. 18, pp. 1016-1024, 1999.

[12] N.Karssemeijer – *"Adaptive Noise Equalisation and Recognition of Microcalcification Clusters in Mammograms",* in International Journal of Pattern Recognition and Artificial Intelligence, vol. 7, pp. 1357-1376, 1992.

[13] N.Karssemeijer – *"Stochastic Model for Automated Detection of Calcifications in Digital Mammograms"*, in Image and Vision Computing, vol. 10, pp, 369-375, 1992.

[14] N.Karssemeijer, and G.M. te Brake – *"Detection of Stellate Distortions in Mammograms"*, in IEEE Transactions on Medical Imaging, vol. 15, pp. 611-619, 1996.

[15] P. Kornprobst, R. Deriche, and G. Aubert – *"Nonlinear Operators in Image Restoration"*, in Computer Vision and Pattern Recognition 1997, pp. 325-330, 1997.

[16] P. Kovesi -- *"Image Features from Phase Congruency"*, in Videre: Journal of Computer Vision Research, vol. 1, 1999.

[17] M.G. Linguraru, J.M. Brady, and M. Yam – *"Filtering h_{int} Images for the Detection of Microcalcifications"*, in W. Niessen, M. Viergever editors, Medical Image Computing and Computer-Assisted Intervention 2001, Lecture Notes in Computer Science, vol. 2208, pp. 629-636, Springer-Verlag Berlin Heidelberg, 2001.

[18] M.G. Linguraru, J.M. Brady, T. Kadir and M. Yam – *"A Novel Method to Detect Microcalcifications for Early Signs of Breast Cancer"*, in V.L. Patel, R. Rogers and R. Haux editors, Medinfo2001, pp. 946, IOS Press, Amsterdam, 2001.

[19] K. Marias, C.P. Behrenbruch, M. Brady, S. Parbhoo, and A. Seifalian, *"Multi-Scale Landmark Selection for Improved Registration of temporal Mammograms"*, in M.J. Yaffe editor, International Workshop on Digital Mammography 2000, pp. 580-586, Medical Physics Publishing Madison, 2000.

[20] R.M. Nishikawa, M.L. Giger, C.J. Vyborny, and R.A. Schmidt – *"Computer-Aided Detection of Clustered Microcalcifications: an Improved Method for Grouping Detected Signals"*, in Medical Physics, vol. 20, pp. 1661-1666, 1993.

[21] P. Perona, and J. Malik – *"Scale-space and edge detection using anisotropic diffusion"* in IEEE Transactions on Medical Imaging, vol. 15, pp. 611-619, 1996.

[22] B. Sahiner, H.P. Chan, N. Petrick, and M.A. Helvie – *"Computerized Characterization of Masses on Mammograms: The Rubber BAnd Straightening TRansform and Texture Analysis"*, in Medical Physics, vol. 25, pp. 516-526, 1998.

[23] M.R. Spiegel -- *Probability an Statistics*, Mc-Graw-Hill Book Company, 1975.

[24] J. Weickert – *"Theoretical Foundations of Anisotropic Diffusion in Image Processing"*, in W. Kropatsch, R. Klette and F. Solina editors, Theoretical Foundations of Computer Vision, vol. 11, pp. 221-236, 1996.

[25] J. Weickert – *"A review of nonlinear diffusion filtering"*, in B. ter Haar Romeny, L. Florack, J. Koenderink, and M. Viergever, editors, Scale-Space Theory in Computer Vision, Lecture Notes in Computer Science, vol. 1252, pp. 3-28, Springer Berlin, 1997.

[26] M. Yam, J.M. Brady, R.P. Highnam, and R. English – *"Denoising h_{int} Surfaces: a Physics Based Approach "*, in Medical Image Computing and Computer-Assisted Intervention 1999, pp 227-234, Springer, 1999.

[27] M. Yam, J.M. Brady, R.P. Highnam, and R. English – *"Detecting calcifications in mammograms using the h_{int} representation"*, in Computer Assisted Radiology and Surgery, pp 373-377, Elsevier, 1999.